J Biol Inorg Chem (2006) 11:769–782
DOI 10.1007/s00775-006-0124-7

ORIGINAL PAPER

Synthesis and biological evaluation of tricarbonyl Re(I) and Tc(I) complexes anchored by poly(azolyl)borates: application on the design of radiopharmaceuticals for the targeting of 5-HT_{1A} receptors

Raquel Garcia · Lurdes Gano · Leonor Maria · António Paulo · Isabel Santos · Hartmut Spies

Received: 6 April 2006 / Accepted: 31 May 2006 / Published online: 6 July 2006

Abstract The building blocks *fac*-[^{99m}Tc{κ^3-HB(tim^{Me})$_3$}(CO)$_3$] and *fac*-[^{99m}Tc{κ^3-R(μ-H)B(tim^{Me})$_2$}(CO)$_3$] [R is H (**4a**), Ph (**5a**); tim^{Me} is 2-mercapto-1-methylimidazolyl] were obtained almost quantitatively by reacting *fac*-[^{99m}Tc(CO)$_3$(H$_2$O)$_3$]$^+$ with the corresponding scorpionate. These compounds cross the intact blood–brain barrier in mice, with significant retention in the case of **4a** and **5a**. Using **4a** as the lead structure, we have synthesized the functionalized complexes *fac*-[M{κ^3-H(μ-H)B(tim$^{Bu\text{-}pip}$)$_2$}(CO)$_3$] [M is Re (**8**), ^{99m}Tc (**8a**); tim$^{Bu\text{-}pip}$ is methyl[4-((2-methoxyphenyl)-1-piperazinyl)butyl](2-mercapto-1-methylimidazol-5-yl)methan amide] and *fac*-[M{κ^3-H(μ-H)B(tim^{Me})(tim$^{Bu\text{-}pip}$)}(CO)$_3$] [M is Re (**9**), ^{99m}Tc (**9a**)] and evaluated their potential as radioactive probes for the targeting of brain 5-HT_{1A} serotonergic receptors. The Re complexes exhibit excellent affinity [IC_{50}=0.172 ± 0.003 nM (**8**); IC_{50}=0.65 ± 0.01 nM (**9**)] for the 5-HT_{1A} receptor. The radioactive congeners (^{99m}Tc) have shown an initial brain uptake of 1.38 ± 0.46%ID g^{-1} (**8a**) and 0.43 ± 0.12%ID g^{-1} (**9a**), but suffer from a relatively fast washout.

Keywords Technetium · Rhenium · Poly(azolyl)borates · 5-HT_{1A} receptor · Bivalent approach

R. Garcia · L. Gano · L. Maria · A. Paulo · I. Santos (✉)
Departamento de Química, ITN, Estrada Nacional 10,
2686-953 Sacavém Codex, Portugal
e-mail: isantos@itn.pt

H. Spies
Institute of Bioinorganic and Radiopharmaceutical Chemistry, Forschungszentrum Rossendorf,
01314 Dresden, Germany

Introduction

In the past few years, great research effort has been devoted to the finding of ^{99m}Tc complexes capable of selectively recognizing central nervous system (CNS) receptors and transporters [1]. In this field, the design of ^{99m}Tc radioactive probes for the targeting of central 5-hydroxytryptamine (5-HT_{1A}) receptors has received considerable attention, as this subtype of serotonergic receptors are implicated in major neuropsychiatric disorders such as schizophrenia, anxiety and depression [2].

Mapping and quantification of 5-HT_{1A} receptors in the human brain by positron emission tomography (PET) is already feasible through the use of the radioligand [carbonyl-^{11}C]WAY-100635 ([*N*-(2-(1-(4-(2-methoxyphenyl)-piperazinyl)ethyl))-*N*-(2-pyridinyl) cyclohexanecarboxamide]) [3–6]. However, the widespread availability of single-photon-emission tomography (SPECT) facilities in comparison with that of PET facilities, the almost ideal properties of ^{99m}Tc for SPECT imaging and its availability still justify the interest in ^{99m}Tc complexes specific for 5-HT_{1A} receptors.

Most of the studies on ^{99m}Tc complexes for targeting 5-HT_{1A} receptors have been focused on fragments of WAY-100635, profiting from the tolerance of replacing the pyridinyl amide group by other substituents. Until now, ^{99m}Tc(V) monooxo complexes anchored by tetradentate ligands, [3+1] mixed-ligand M(V) oxocomplexes or [4+1] mixed-ligand M(III) complexes have been the most explored systems [7–13]. Compounds containing the [Tc ≡ N]$^{2+}$ and the *fac*-[^{99m}Tc(CO)$_3$]$^+$ core have also been applied in the design of ^{99m}Tc agents for imaging 5-HT_{1A} receptors, taking advantage

of the recently introduced labelling methodologies based on these metal fragments [14–17]. In spite of these efforts, none of the complexes evaluated have proved to be promising candidates for imaging human 5-HT_{1A} receptors, essentially owing to their poor brain uptake.

The availability of the organometallic *fac*-[^{99m}Tc$(CO)_3(H_2O)_3]^+$ (**1**) synthon brought new hopes and perspectives to the research on ^{99m}Tc complexes for molecular imaging applications, as its unique features allow the use of a large variety of ligands and/or donor sets [15–21]. Using this organometallic approach, we have focused on soft and hard scorpionates as bifunctional chelators for the *fac*-$[M(CO)_3]^+$ moieties (M is Re, Tc). Our previous chemical studies with poly(mercaptoimidazolyl)borates, at macroscopic level (Re and ^{99}Tc), demonstrated that these soft scorpionates act as tridentate ligands either in the solid state or in solution, as confirmed by X-ray diffraction and NMR analysis of *fac*-[Re{κ^3-HB(tim^{Me})$_3$}$(CO)_3$] (**3**) and *fac*-[Re{κ^3-R(μ-H)B(tim^{Me})$_2$}$(CO)_3$] [R is H (**4**), Ph (**5**); tim^{Me} is 2-mercapto-1-methylimidazolyl] [21–23]. All these complexes display a remarkable resistance towards hydrolysis or oxidation processes, even those containing coordinated agostic hydrides, which is the smallest possible ligand in coordination and organometallic chemistry. Being small-sized, neutral and lipophilic, complexes **3–5** can be considered relevant building blocks to design radiopharmaceuticals for CNS receptor imaging.

In this work we describe the synthesis, characterization and biological evaluation of the radioactive congeners of **3–5**, *fac*-[^{99m}Tc{κ^3-HB(tim^{Me})$_3$}$(CO)_3$] (**3a**) and *fac*-[^{99m}Tc{κ^3-R(μ-H)B(tim^{Me})$_2$}$(CO)_3$] [R is H (**4a**), Ph (**5a**)], which were obtained by reacting *fac*-[^{99m}Tc$(CO)_3(H_2O)_3]^+$ (**1**) with Na[HB(tim^{Me})$_3$] (**L**^{1}), Na[H_2B(tim^{Me})$_2$] (**L**^{2}) and Li[H(Ph)B(tim^{Me})$_2$] (**L**^{3}), respectively. Studies performed with the hard scorpionates Na[HB(3,5-Me_2pz)$_3$] (**L**^{4}) and Na[H_2B(3,5-Me_2pz)$_2$] (**L**^{5}) (pz is pyrazolyl) at the macroscopic and no-carrier-added (NCA) level are also reported.

To further demonstrate the utility of our building blocks, the framework of **4a** was coupled to a fragment of WAY-100635 at the 5-position of the azole ring(s). The synthesis, characterization and biological evaluation of the resulting complexes *fac*-[M{κ^3-H(μ-H)B($tim^{Bu\text{-}pip}$)$_2$}$(CO)_3$] [M is Re (**8**), ^{99m}Tc (**8a**); $tim^{Bu\text{-}pip}$ is methyl[4-((2-methoxyphenyl)-1-piperazinyl)butyl](2-mercapto-1-methylimidazol-5-yl)methanamide] and *fac*-[M{κ^3-H(μ-H)B(tim^{Me})($tim^{Bu\text{-}pip}$)}$(CO)_3$] [M is Re (**9**), ^{99m}Tc (**9a**)] is described inhere. The affinity and selectivity of the rhenium complexes **8** and **9** for 5-HT_{1A} receptors, as well as the pharmacokinetics and brain uptake of the corresponding ^{99m}Tc complexes **8a** and **9a**, is also discussed in this work.

Materials and methods

All chemicals and solvents were of reagent grade and were used without purification unless stated otherwise. ^{1}H, ^{11}C and ^{11}B NMR spectra were recorded using a Varian Unity 300-MHz spectrometer; the NMR spectra were run at room temperature, except when indicated. ^{1}H and ^{11}C chemical shifts were referenced to the residual solvent resonances relative to tetramethylsilane. ^{11}B NMR chemical shifts were referenced to an external alkaline solution of $NaBH_4$. IR spectra were recorded as KBr pellets with a Perkin-Elmer 577 spectrometer. C, H and N analyses were performed using an EA 110 CE Instruments automatic analyser. All the new compounds, except Na[H_2B($tim^{Bu\text{-}pip}$)$_2$] (**L**^{6}) and Na[H_2B(tim^{Me})($tim^{Bu\text{-}pip}$)] (**L**^{7}), were characterized by Fourier transform ion cyclotron resonance mass spectrometry (FT/ICR–MS) or electrospray ionization mass spectrometry (ESI–MS). **L**^{1} [24], **L**^{2} [25], **L**^{3} [22], **L**^{4}, **L**^{5} [26] and the $timH^{Bu\text{-}pip}$ [27] were prepared according to published methods. The radioactive precursor **1** was prepared using an IsoLink kit (Malinckrodt). The starting material (NE-t_4)$_2$[Re$(CO)_3Br_3$] (**2**) [28], the model rhenium complexes **3**, **4**, **5** and *fac*-[Re{κ^3-HB(3,5-Me_2pz)$_3$}$(CO)_3$] (**6**) were prepared as described elsewhere [21–23, 29]. Na[$^{99m}TcO_4$] was eluted from a ^{99}Mo/^{99m}Tc generator, using 0.9% saline. High-performance liquid chromatography (HPLC) analysis of the Re and ^{99m}Tc complexes was performed with a PerkinElmer LC pump 200 coupled to an LC 290 tunable UV/vis detector and to a Berthold LB-507A radiometric detector. Separations were achieved on a Nucleosil column (10 μm, 250 mm × 4 mm), using a flow rate of 1 mL min^{-1}; UV detection, 254 nm; eluents: A, aqueous 0.1% CF_3COOH solution; B, methanol or acetonitrile; method: *t*=0–3 min, 0% B; 3–3.1 min, 0–25% B; 3.1–9 min, 25% B; 9–9.1 min, 25–34% B; 9.1–20 min, 34–100% B; 20–22 min, 100% B; 22–22.1 min, 100–0% B; 22.1–30 min, 0 % B.

Synthesis of Na[H_2B($tim^{Bu\text{-}pip}$)$_2$] (**L**^{6})

To a suspension of $NaBH_4$ (16 mg, 0.42 mmol) in tetrahydrofuran (THF) was added a solution of $timH^{Bu\text{-}pip}$ (420 mg, 1.01 mmol) in THF and the reaction mixture was refluxed for 60 h. After this time, the solvent was removed under vacuum and the

compound was purified by successive recrystallizations from THF/*n*-hexane. Yield: 286 mg, 78%. ^{1}H NMR (CD_3CN, δ): 7.43 (s, CH, 2H), 6.93–6.86 (m, aromatic, 8H), 3.78 (s, OCH_3, 6H), 3.52 (t, CH_2, 4H), 3.49 (s, CH_3, 6H), 3.027 (s, NCH_3, 6H), 2.97 (br, NCH_2, 8H), 2.50 (br, NCH_2, 8H), 2.34 (t, CH_2, 4H), 1.61 (m, CH_2, 4H), 1.47 (m, CH_2, 4H). ^{11}B NMR (CD_3CN, δ): 32.4 (br). ^{13}C NMR (CD_3CN, δ) : 24.6, 26.2, 33.5, 51.4, 54.3, 55.8, 58.7, 68.2, 112.6, 119.0, 121.3, 121.9, 123.4, 129.5, 142.8, 153.3, 162.5, 167.3. IR (KBr, ν/cm^{-1}): ν(BH) 2,412; ν(C=O) 1,621. Anal. Calcd. for $C_{42}H_{62}N_{10}O_4S_2BNa$: C, 58.08; H, 7.11; N, 16.13. Found: C, 57.84; H, 7.26; N, 16.04.

Synthesis of Na[$H_2B(tim^{Me})(tim^{Bu\text{-}pip})$] (**L^7**)

To a stirred suspension of $NaBH_4$ (35 mg, 0.93 mmol) in THF at 50 °C was added dropwise a solution of $timH^{Me}$ (100 mg, 0.88 mmol) and $timH^{Bu\text{-}pip}$ (363 mg, 0.87 mmol) in the same solvent. The resulting mixture was stirred overnight at this temperature. After cooling to room temperature and concentration under vacuum, addition of *n*-hexane led to the formation of a white precipitate which was formulated as **L^7**. Further purification of **L^7** was attempted by successive recrystallizations from THF/*n*-hexane. However, as indicated by NMR spectroscopy, **L^7** was always slightly contaminated (less than 3%) with the symmetric **L^2**. Yield: 103.4 mg, 21.1 %. ^{1}H NMR (300 MHz, CD_3CN, δ):7.49 (s, CH, 1H), 7.01 (d, CH, J_{H-H}=2.4 Hz, 1H), 6.94–6.89 (m, aromatic and CH, 5H), 6.58 (d, CH, J_{H-H}=2.1 Hz, 1H), 3.79 (s, OCH_3, 3H), 3.51 (s, CH_3, 3H), 3.49 (s, CH_3, 3H), 3.44 (t, CH_2, 2H), 3.02 (s, NCH_3, 3H), 2.97 (br, NCH_2, 4H), 2.50 (br, NCH_2, 4H), 2.34 (m, CH_2, 2H), 1.61 (m, CH_2, 2H), 1.46 (m, CH_2, 2H). ^{11}B NMR (CD_3CN, δ):32.9 (t). IR (KBr, ν/cm^{-1}): ν(BH) 2,414; ν(C=O) 1,627.

Synthesis of *fac*-[Re{κ^3-(μ-OH)BH(3,5-Me_2pz)}$(CO)_3$] (**7**)

To a solution of **2** (100 mg, 0.13 mmol) in water was added solid **L^5** (29 mg, 0.13 mmol), and the resulting mixture was stirred at room temperature for 2 h. After this time, the white precipitate formed was separated by centrifugation, dried under vacuum and applied on a silica gel column, which was eluted with 50% CH_2Cl_2/*n*-hexane. Removal of the solvent from the collected fractions gave compound **7** as a pale yellow solid. Yield: 12 mg, 19%. ^{1}H NMR ($CDCl_3$, δ): 5.77 (s, CH, 2H), 4.20 (br, BH, 1H), 2.74 (s, OH, 1H), 2.33 (s, CH_3, 6H), 2.29 (s, CH_3, 6H). ^{11}B NMR ($CDCl_3$, δ): 34.2 (d, J_{B-H}=121 Hz). IR (KBr, ν/cm^{-1}): ν(OH) 3,449; ν(BH) 2,514; ν(C ≡ O) 1,888, 1,916, 2,026. FT/ICR–MS (+) (*m*/*z*): 490 [M+H]$^+$.

Synthesis of *fac*-[Re{κ^3-H(μ-H)($tim^{Bu\text{-}pip}$)$_2$}$(CO)_3$] (**8**)

A solution of **L^6** (60 mg, 0.072 mmol) in MeOH was added to a stirred solution of **2** (55 mg, 0.071 mmol) in the same solvent. After stirring for 6 h at room temperature, the solvent was evaporated to dryness. The yellow residue was applied on a silica gel column which was eluted with 10% MeOH in CH_2Cl_2. Removal of the solvent from the collected fractions yielded **8** as a pale yellow microcrystalline solid. Yield: 31 mg, 39%. ^{1}H NMR ($CDCl_3$, 40 °C, δ): 7.01–6.83 (m, aromatic and CH, 10H), 3.84 (s, OCH_3, 6H), 3.62 (s, CH_3, 6H), 3.47 (t, CH_2, 4H), 3.11 (br, CH_2N, 8H), 3.06 (s, CH_3N, 6H), 2.69 (br, CH_2N, 8H), 2.50 (t, CH_2, 4H), 1.65– 1.55 (m, CH_2, 8H), –6.58 (br, 1H, B–H···Re). ^{11}B NMR ($CDCl_3$, 40 °C, δ): 32.3 (br). ^{13}C NMR ($CDCl_3$, δ): 23.6, 25.0, 25.3, 33.8, 37.4, 47.8, 50.2, 53.3, 55.3, 58.0, 111.1, 118.2, 121.0, 123.2, 128.1, 140.8, 152.2, 159.9, 167.5, 190.6, 191.9. IR (KBr, ν/cm^{-1}): ν(B–H) 2,449 (w); ν(B–H···Re) 2,093 (w); ν(C ≡ O) 2,025 (vs), 1,910vs; ν(C=O) 1,634. ESI–MS (+) (*m*/*z*): 1,117.4 [M–H]$^+$. Anal. Calcd. for $C_{45}H_{62}N_{10}O_7S_2BRe$: C, 48.43; H, 5.56; N, 12.56. Found: C, 47.72; H, 5.82; N, 12.22.

Synthesis of *fac*-[Re{κ^3-H(μ-H)(tim^{Me})($tim^{Bu\text{-}pip}$)}$(CO)_3$] (**9**)

A solution of **L^7** (53 mg, 0.09 mmol) in MeOH was added to a solution of **2** (72 mg, 0.09 mmol) in the same solvent. After stirring for 3 h at room temperature, the solvent was evaporated to dryness. The yellow oil was chromatographed on a silica gel column with MeOH/CH_2Cl_2/ammonia (3:90:0.01) to afford a pale yellow solid which was formulated as **9**. Yield: 14 mg, 18 %. ^{1}H NMR (CD_3CN, 70 °C, δ):7.15 (s, CH, 1H), 7.07 (d, CH, 1H, J_{H-H} =2.1 Hz), 6.96–6.88 (m, aromatic and CH, 5H), 3.80 (s, OCH_3, 3H), 3.56 (s, CH_3, 3H), 3.51 (s, CH_3, 3H), 3.45 (t, CH_2, 2H), 3.01 (m, CH_3N and NCH_2, 7H), 2.51 (br, NCH_2, 4H), 2.33 (t, CH_2, 2H), 1.62 (m, CH_2, 2H), 1.47 (m, CH_2, 2H), –6.61 (br, 1H, B–H···Re). ^{11}B NMR (CD_3CN, δ): 34.0 (br). ^{13}C NMR (CD_3CN, δ): 24.3, 25.5, 27.6, 34.2, 35.2, 51.2, 54.2, 55.9, 58.5, 112.6, 119.0, 121.9, 122.4, 123.5, 124.9, 129.6, 142.5, 153.3, 160.7, 164.4, 166.6, 192.2, 194.0. IR (KBr, ν/cm^{-1}): ν(B–H) 2,442 (w); ν(B–H···Re) 2,167 (w), 2,091 (w); ν(C ≡ O) 2,023 (vs), 1,906 (vs); ν(C=O) 1,632.

ESI–MS (+) (*m*/*z*): 814.84 $[M]^+$. Anal. Calcd. for $C_{28}H_{37}N_7O_5S_2BRe$: C, 41.32; H, 4.59; N, 12.05. Found: C, 40.98; H, 4.64; N, 11.94.

Synthesis of the ^{99m}Tc complexes (**3a**–**5a**, **8a** and **9a**): general method

A volume of 900 μl (3–4 mCi) of the organometallic precursor *fac*-$[^{99m}Tc(OH_2)_3(CO)_3]^+$, 100 μL of 10^{-4} or 10^{-3} M aqueous solution of the poly(mercaptoimidazolyl)borate ligands (**L**^{1}–**L**^{3} or **L**^{6} and **L**^{7}) and 150 μL of propylene glycol were placed in a 10-mL glass vial under nitrogen. The vial was then heated to 75 °C for 30 min, cooled on an ice bath and the final solution analysed by HPLC. Unlike the other complexes, **9a** was purified by gradient HPLC (100% aqueous 0.1% CF_3COOH solution → 100% CH_3CN) using a Nucleosil column (10 μm, 250 mm × 4 mm). Before HPLC purification, **9a** was extracted with CH_2Cl_2, the solvent was removed under N_2 and the radioactive residue redissolved in 100 μL of ethanol.

The attempts to prepare ^{99m}Tc complexes with the poly(pyrazolyl)borates **L**^{4} and **L**^{5} were performed as described before for the poly(mercaptoimidazolyl) borate ^{99m}Tc tricarbonyl complexes.

Octanol–water partition coefficient

The log$P_{o/w}$ values of complexes **3a**–**5a**, **8a** and **9a** were determined by the multiple back extraction method [30] under physiological conditions (*n*-octanol/0.1 M phosphate-buffered saline, PBS, pH 7.4).

Cysteine and histidine challenge

A volume of 100 μL of **3a**–**5a**, **8a** and **9a** was added to 900 μL of 10^{-3} M cysteine or histidine solutions in PBS at pH 7.4. The samples were incubated at 37 °C and aliquots were analysed by HPLC at different time points.

In vitro plasma stability and plasmatic protein binding

A volume of 100 μL of **3a**–**5a** was added to 500 μL of human plasma and incubated at 37 °C. After incubation (0, 1, 2 and 4 h), aliquots were taken and the plasmatic proteins precipitated with 1 mL of ethanol. The plasma was centrifuged at 3,000 rpm for 15 min at 4 °C and the supernatant (protein-free plasma) was analysed by HPLC. The pellet was washed twice with 500 μL of PBS buffer, followed by centrifugation at 2,000 rpm for 10 min. The activity in the sediment was compared with the activity in the supernatant to calculate the percentage of complex bound to proteins.

Biodistribution studies

The in vivo behaviour of complexes **3a**–**5a**, **8a** and **9a** was evaluated in groups of five female CD-1 mice (randomly bred, Charles River) weighing approximately 20–25 g each. Animals were intravenously injected with 100 μL (1.5–8.0 MBq) of each preparation via the tail vein and were maintained on a normal diet ad libitum. Mice were killed by cervical dislocation at 5 min, 1 h and 2 h after injection (p.i). The injected radioactive dose and the radioactivity remaining in the animal after it had been killed were measured with a dose calibrator (Aloka, Curiemeter IGC-3, Tokyo, Japan). The difference between the radioactivity in the injected and killed animal was assumed to be due to total excretion from whole-body animal. Blood samples were taken by cardiac puncture at the time the animal was killed. Tissue samples of the main organs were then removed, weighed and counted in a gamma counter (Berthold). Biodistribution results were expressed as a percentage of the injected dose (%ID) per organ and/or per gram of tissue. For blood, bone and muscle, total activity was calculated assuming that these organs constitute 6, 10 and 40% of the total weight, respectively. The remaining activity in the carcass was also measured with a dose calibrator. For complexes **8a** and **9a** the residual blood remaining in capillaries of brain was calculated on the basis of the brain and blood uptake of ^{99m}Tc-DTPA determined in the same animal model and under identical experimental conditions. The blood activity-to-volume ratio was determined and the residual blood retained in the excised brain calculated. The latter was used to correct the brain uptake found for **8a** and **9a**. Blood samples, collected at the time the animal was killed, were centrifuged, the serum was separated and treated with ethanol to precipitate the proteins and the supernatant was analysed by HPLC, as described before for the in vitro plasma stability evaluation.

Receptor binding assays on rat brain homogenates

The receptor binding assays were performed as described elsewhere [13]. For the 5-HT_{1A} receptor binding assay [^{3}H]8-OH-DPAT (NEN, 4.6 TBq mmol^{-1}) as specific radioligand and rat hippocampus homogenate were used. Rat cortex homogenates were used for the 5-HT_{2A} receptor binding assay with [^{3}H]ketanserin (NEN, 2.3 TBq mmol^{-1}) as a specific radioligand.

The incubation step of binding assays was terminated by rapid filtration through GF/B glass fibre filters (Whatman) using a 30-port Brandell cell harvester. The filters were rapidly washed with 4-mL portions of ice-cold buffer, transferred into 4 mL scintillation liquid (Ultima Gold, Packard) and analysed for radioactivity by scintillation counting (Beckmann-LS 600-LL).

Results

Synthesis and characterization of the ^{99m}Tc building blocks

Following our previous studies at the macroscopic level [21–23], we explored the possibility of preparing at the NCA level (^{99m}Tc) tricarbonyl complexes anchored by the poly(mercaptoimidazolyl)borates **L^1**– **L^3** (Structure 1).

In aqueous solution, compounds **L^1**–**L^3** react at 75 °C with the precursor **1**, yielding **3a**, **4a** and **5a**, respectively (Scheme 1). These reactions are almost quantitative (more than 98%) for concentrations of **L^1**–**L^3** as low as 10^{-5} mol L^{-1}. The chemical identity of **3a**–**5a** was confirmed by comparison of their HPLC profiles with those of the corresponding rhenium complexes (**3**–**5**), previously synthesized and charac-

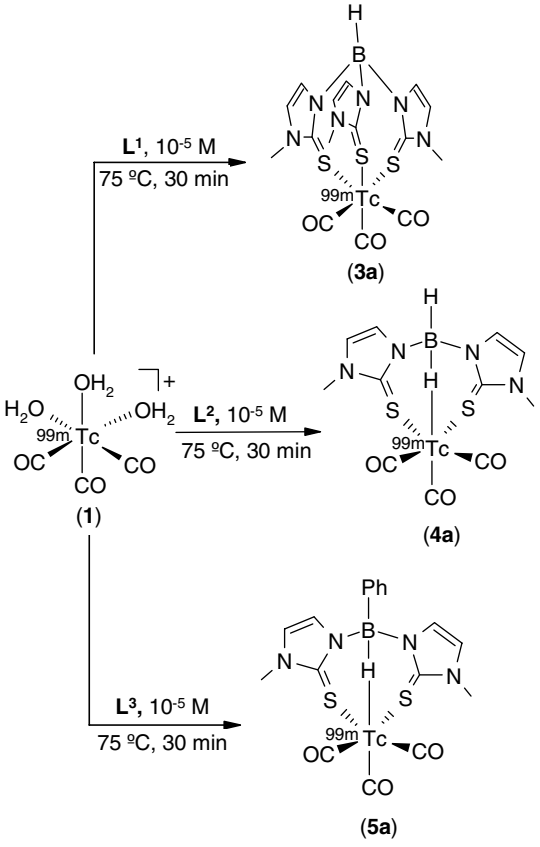

Scheme 1 Synthesis of the ^{99m}Tc building blocks

Poly(mercaptoimidazolyl)borates

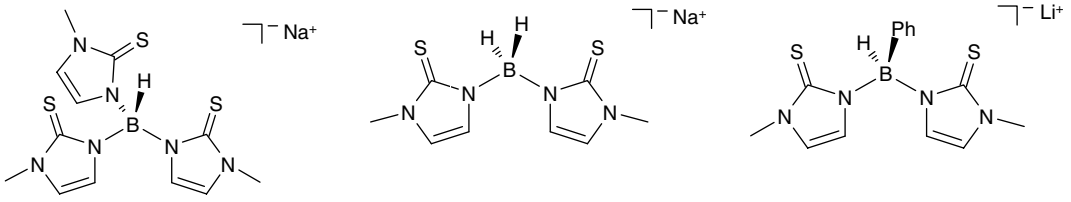

Na[HB(tim^{Me})$_3$] (**L^1**) Na[H$_2$B(tim^{Me})$_2$] (**L^2**) Li[H(Ph)B(tim^{Me})$_2$] (**L^3**)

Poly(pyrazolyl)borates

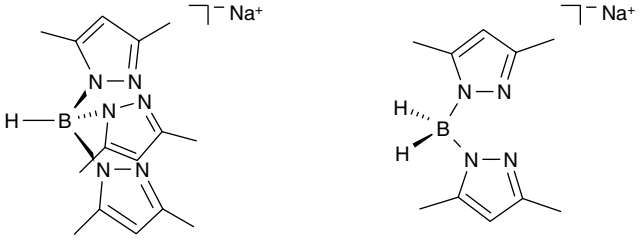

Na[HB(3,5-Me$_2$pz)$_3$] (**L^4**) Na[H$_2$B(3,5-Me$_2$pz)$_2$] (**L^5**)

Structure 1

Table 1 High-performance liquid chromatography retention time (t_R) and log$P_{o/w}$ values for *fac*-[^{99m}Tc{κ^3-HB(tim^{Me})$_3$}(CO)$_3$] (**3a**) and *fac*-[^{99m}Tc{κ^3-R(μ-H)B(tim^{Me})$_2$}(CO)$_3$] [R is H (**4a**), Ph (**5a**)] (tim^{Me} is 2-mercapto-1-methylimidazolyl)

Complex	t_R (min)	log$P_{o/w}$
3a	22.03 (21.4)[a]	1.50 ± 0.01
4a	22.4 (21.8)[a]	1.64 ± 0.08
5a	22.03 (21.7)[a]	1.59 ± 0.08

[a]The values in *parentheses* are for the corresponding Re complexes **3–5**

terized in the solid state and in solution [21, 22]. Table 1 summarizes the octanol–water partition coefficient expressed as log$P_{o/w}$ and the retention time for complexes **3a–5a**.

The excellent coordination capability towards the *fac*-[^{99m}Tc(CO)$_3$]$^+$ moiety found for poly(mercaptoimidazolyl)borates led us to extend our studies to the related pyrazolyl-containing ligands **L^4** and **L^5** (Structure 1). In the literature, it was already reported that reactions of these poly(pyrazolyl)borates with [M(CO)$_5$X] (M is Re, ^{99}Tc; X is Cl, Br) in an organic medium yield *fac*-[M{κ^3-HB(3,5-Me$_2$pz)$_3$}(CO)$_3$] [M is ^{99}Tc, Re (**6**)] and *fac*-[Re{κ^2-H$_2$B(pz)$_2$}(CO)$_3$(pzH)], respectively [29, 31]. However, the chemistry of **L^4** and **L^5** with the aquo ions *fac*-[M(CO)$_3$(OH$_2$)$_3$]$^+$ [M is ^{99m}Tc (**1**), Re (**2**)] [18], relevant for radiopharmaceutical application, has never been explored.

We have found that **2** reacts with **L^4** and **L^5** in aqueous solution or in organic media (CH$_3$CN or THF) with degradation of the ligands. For **L^4**, no well-defined species could be identified, but in the reactions with **L^5**, complex **7** was isolated and fully characterized (Scheme 2).

Compound **7** is a pale yellow microcrystalline solid, soluble in most common organic solvents and insoluble in water, which was recovered by column chromatography in a relatively low yield (18 %). Its formulation was based on IR, ^{1}H and ^{11}B NMR spectroscopy and on mass spectrometry. The IR spectrum of **7** displays three very strong ν(CO) bands in the 2,026–1,888-cm^{-1} range, confirming a *fac*-coordination geometry. There is a strong band at 3,449 cm^{-1}, assigned to the ν(OH) stretching vibration, which corroborates the presence of the heteroscorpionate [H(HO)B(3,5-Me$_2$pz)$_2$]$^-$. Consistently, the IR spectrum of **7** shows only one single ν(BH)$_{terminal}$ band at 2,514 cm^{-1}. The absence of high-field-shifted Re···H–B resonances in the ^{1}H NMR spectrum and the presence of a well-defined doublet at 34.2 ppm (J_{B-H}=121 Hz) in the ^{11}B NMR spectrum are also in agreement with the formulation proposed for **7**.

Despite the results obtained with rhenium, we reacted **1** with **L^4** and **L^5**, using the experimental conditions described before for the synthesis of the poly(mercaptoimidazolyl)borate tricarbonyl complexes **3a–5a**. Compound **1** reacts with **L^4** and **L^5** with rather unfavourable kinetics, leading to a mixture of radiochemical species. As exemplified for **L^5** in Fig. 1, the main interesting feature of these reactions was the formation of a major radiochemical species appearing at t_R=22.5 min, which does not correspond to the ^{99m}Tc analogues of **6** (t_R =26.2 min) and **7** (t_R=24.1 min). No additional efforts were made to assign the chemical structure of the major ^{99m}Tc complex, as this species could hardly be considered relevant for further application in the labelling of CNS-receptor ligands.

In vitro and in vivo evaluation of ^{99m}Tc building blocks

The building blocks anchored by poly(mercaptoimidazolyl)borates, **3a–5a**, which were obtained as

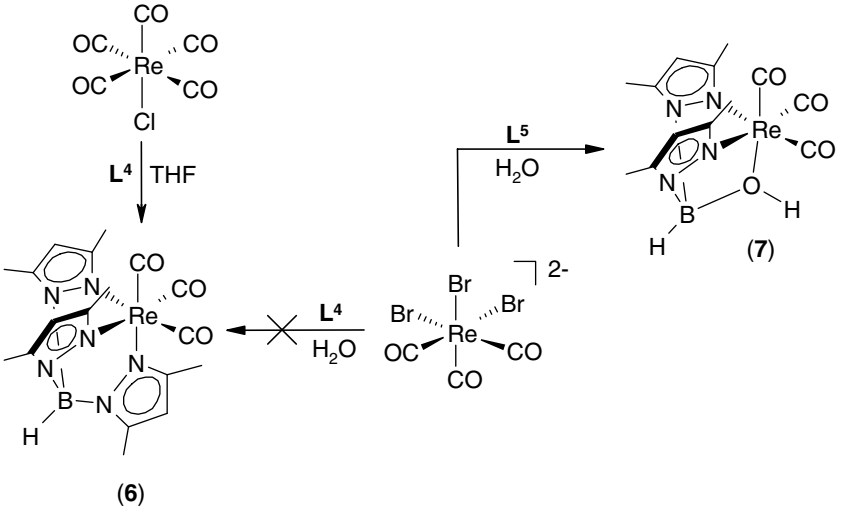

Scheme 2 Reactions of *fac*-[Re(CO)$_3$Br$_3$]$^{2-}$ with Na[HB(3,5-Me$_2$pz)$_3$] (**L^4**) and Na[H$_2$B(3,5-Me$_2$pz)$_2$] (**L^5**) (pz is pyrazolyl)

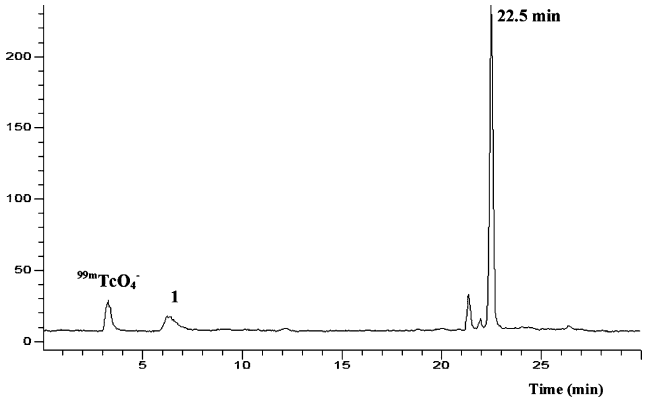

Fig. 1 High-performance liquid chromatography (*HPLC*) chromatogram for the reaction of *fac*-$[Tc(CO)_3(OH_2)_3]^+$ with $Na[H_2B(3,5\text{-}Me_2pz)_2]$ ($\mathbf{L^5}$) (pz is pyrazolyl)

well-defined and chemically identified species in high radiochemical purity and high specific activity, were evaluated in vitro and in vivo.

Complexes **3a–5a** display a great stability in vitro under physiological conditions, namely in PBS (pH 7.4) and in human plasma, as indicated by HPLC analysis. The assays with human plasma were also used to determine the percentage of protein binding, and the values found were 16.0 ± 1.3, 28.5 ± 1.8 and 14.5 ± 0.9% for **3a**, **4a** and **5a,** respectively. For all complexes, no reoxidation to pertechnetate could be observed, even after 24 h of incubation. These observations have shown that, under physiological conditions, the presence of B–H agostic hydrides does not compromise the in vitro robustness of **4a** and **5a**.

As shown in Fig. 2, significant differences were observed in challenge experiments with 1 mM histidine and cysteine solutions at 37 °C. Complex **3a** showed almost no degradation or *trans* chelation in the presence of both substrates. By contrast, **4a** and **5a** displayed a greater reactivity towards cysteine (Fig. 2). After 6 h of incubation in the presence of an excess of cysteine, only 16% of **4a** and 7% of **5a** remained intact. Most probably, these differences may be accounted by an eventual attack of the substrate on the M···H–B agostic interaction. Nevertheless, the stability of **3a–5a** under physiological conditions and their moderate to high robustness in the presence of histidine, one of the most powerful ligands for the *fac*-$[^{99m}Tc(CO)_3]^+$ moiety, prompted us to pursue the in vivo biological studies.

Biodistribution studies of **3a–5a** were performed in female CD-1 mice, in order to check their ability to cross the blood–brain barrier (BBB). The organ distribution of **3a–5a** as a function of time is summarized in Table 2.

All complexes displayed a relatively fast blood clearance, following the order **3a**>**4a**>**5a**. Only a negligible fraction of the injected radioactivity was retained by the stomach (values between 0.2 and 2.6%ID), demonstrating that **3a–5a** do not undergo in vivo reoxidation to pertechnetate. There is a fast and high hepatic uptake, as expected for lipophilic complexes, mainly excreted through the hepatobiliary system. As a result, the overall excretion rate is relatively slow. The building blocks **3a–5a** can cross the BBB, showing a significant initial brain uptake (1.41 ± 0.09, 2.40 ± 0.32 and 1.52 ± 0.09%ID g^{-1} at 5 min p.i for **3a**, **4a** and **5a**, respectively). Although **3a** suffers from a relatively fast brain washout (0.10 %ID g^{-1}, 2 h p.i), complexes **4a** and **5a** present a reasonable retention in the brain at 2 h p.i. (0.42 and 0.56 %ID g^{-1} for **4a** and **5a**, respectively).

Synthesis and characterization of target-specific Re complexes

On the basis of the physicochemical and biological data discussed earlier for the building blocks **3a–5a**, we considered the lead structure **4a** as the most promising

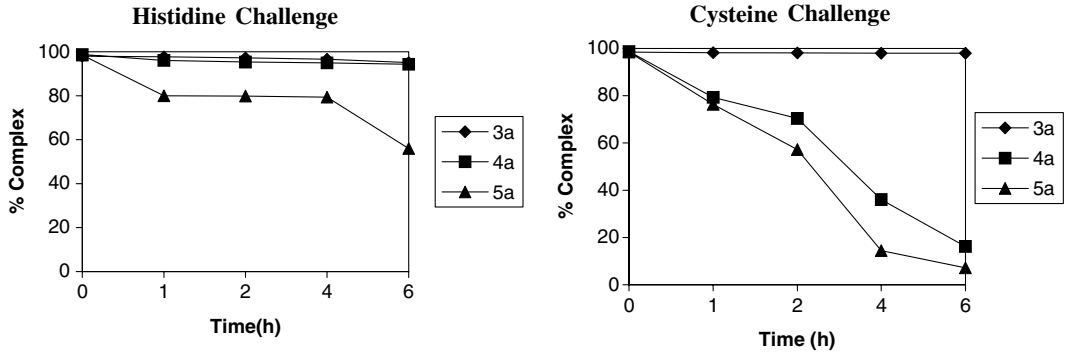

Fig. 2 Stability of *fac*-$[^{99m}Tc\{\kappa^3\text{-}HB(tim^{Me})_3\}(CO)_3]$ (**3a**) and *fac*-$[^{99m}Tc\{\kappa^3\text{-}R(\mu\text{-}H)B(tim^{Me})_2\}(CO)_3]$ [R is H (**4a**), Ph (**5a**)] (tim^{Me} is 2-mercapto-1-methylimidazolyl) in 1mM cysteine and histidine solutions, at 37 °C

Table 2 Biodistribution data of complexes **3a**–**5a** in Charles River mice at 5, 60 and 120 min after injection (*p.i.*) (%ID g^{-1} ± standard deviation)

Time (min)	Brain	Blood	Liver	Kidneys
Complex **3a**				
5	1.41 ± 0.09	1.81 ± 0.27	16.47 ± 2.32	7.2 ± 1.8
60	0.27 ± 0.07	1.20 ± 0.31	26.80 ± 3.81	3.48 ± 0.72
120	0.10 ± 0.02	0.70 ± 0.07	29.41 ± 2.41	2.02 ± 0.25
Complex **4a**				
5	2.40 ± 0.32	3.17 ± 0.62	16.31 ± 2.40	7.57 ± 0.48
60	0.56 ± 0.05	1.42 ± 0.08	24.13 ± 2.93	4.86 ± 0.47
120	0.42 ± 0.04	1.17 ± 0.16	28.31 ± 4.74	3.98 ± 0.61
Complex **5a**				
5	1.52 ± 0.09	3.39 ± 0.39	17.34 ± 1.83	8.84 ± 0.69
60	0.85 ± 0.07	2.35 ± 0.37	18.78 ± 3.62	7.49 ± 1.09
120	0.56 ± 0.08	1.80 ± 0.43	19.41 ± 3.01	6.26 ± 1.24

for further application in the development of ^{99m}Tc complexes for the specific targeting of 5-HT_{1A} receptors. By choosing this lead structure, we have taken into account that **4a** has a favourably small size, while showing an overall brain uptake higher than that of **3a** and comparable to that of **5a**.

As can be seen in Scheme 3, the synthesis of the bifunctional ligand $\mathbf{L^6}$ was performed by reacting $NaBH_4$ with an approximate twofold excess of $timH^{Bu\text{-}pip}$ in refluxing THF. The asymmetric $\mathbf{L^7}$ was prepared in a similar way but using an equimolar mixture of 1-methyl-2-mercaptoimidazole and $timH^{Bu\text{-}pip}$. $timH^{Bu\text{-}pip}$ was synthesized as previously described [32]. The synthesis of $\mathbf{L^6}$ was straightforward and the compound was easily recovered in 78 % yield after recrystallization from THF/*n*-hexane. By contrast, the purification of $\mathbf{L^7}$ was a more demanding task. During the synthesis of $\mathbf{L^7}$, we could not avoid the concomitant formation of the symmetric compound $\mathbf{L^2}$. After several recrystallizations from THF/*n*-hexane, $\mathbf{L^7}$ was obtained slightly contaminated with $\mathbf{L^2}$ (less than 3%). Compounds $\mathbf{L^6}$ and $\mathbf{L^7}$ are microcrystalline solids, water-soluble and resistant towards hydrolysis and air oxidation, and are therefore appropriate for the preparation of radiopharmaceuticals.

As shown in Scheme 4, **2** reacts with $\mathbf{L^6}$ and $\mathbf{L^7}$ to afford **8** and **9**, respectively. The compounds were obtained in low to moderate yields (18–39%), after appropriate purification by column chromatography.

Compounds **8** and **9** are pale yellow solids, and are soluble in most common organic solvents and insoluble in water. Their characterization involved IR, ^{1}H, ^{13}C and ^{11}B NMR spectroscopy, and their formulation was confirmed by mass spectrometry. The positive-ion mass spectra obtained for **8** and **9** showed prominent molecular ion peaks, with isotopic patterns in agreement with the elemental composition of the complexes.

The IR spectra of **8** and **9** display two strong ν(C ≡ O) bands in the range 1,906–2,025 cm^{-1}, typical of complexes with the *fac*-$[Re(CO)_3]^+$ moiety. The weak bands in the range 2,091–2,167 cm^{-1} were assigned to ν(B–H···Re) [21, 22]. These bands are strongly redshifted compared with the $\nu(B–H)_{terminal}$ ones (**8**, 2,449 cm^{-1}; **9**, 2,442 cm^{-1}), which appear at higher energy than the ν(B–H) vibrations in the corresponding free ligands ($\mathbf{L^6}$, 2,412 cm^{-1}; $\mathbf{L^7}$, 2,414 cm^{-1}).

At room temperature and in $CDCl_3$ solution, the ^{1}H and ^{13}C NMR spectra of **8** and **9** show a considerable broadness for some of the resonances, especially for those associated with the piperazinyl moiety and the butylenic spacer. These observations pointed out that **8** and **9** are involved in a dynamic process, and prompted their study by variable-temperature ^{1}H NMR.

As shown in Fig. 3, a fast-limit exchange spectrum was obtained in $CDCl_3$ at 40 °C for **8**. The intensity and multiplicity of the resonances observed in the spectrum of **8** agree with the formulation proposed for this compound. For complex **9**, a fast-limit exchange spectrum could not be obtained in the range of temperatures that can be studied in $CDCl_3$. However, a

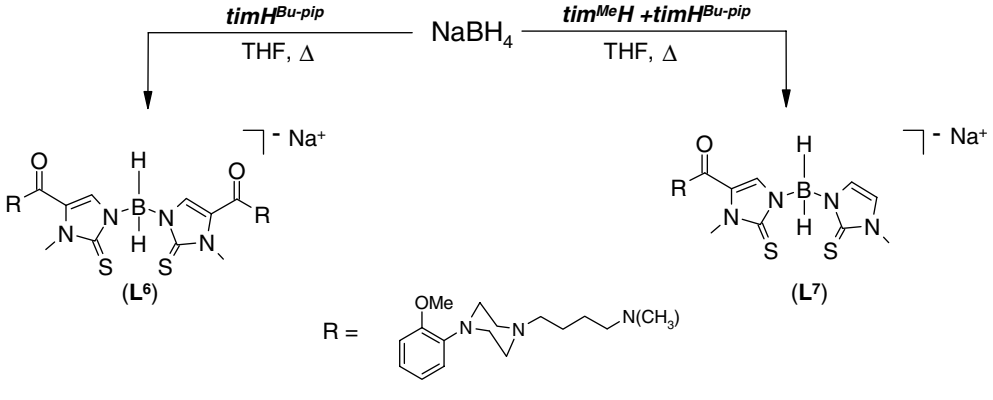

Scheme 3 Synthesis of $Na[H_2B(tim^{Bu\text{-}pip})_2]$ ($\mathbf{L^6}$) and $Na[H_2B(tim^{Me})(tim^{Bu\text{-}pip})]$ ($\mathbf{L^7}$) ($tim^{Bu\text{-}pip}$ is methyl[4-((2-methoxyphenyl) -1-piperazinyl)butyl] (2-mercapto-1-methylimidazol-5-yl)methanamide, tim^{Me} is 2-mercapto-1-methylimidazolyl)

Scheme 4 Synthesis of target-specific Re and ^{99m}Tc complexes

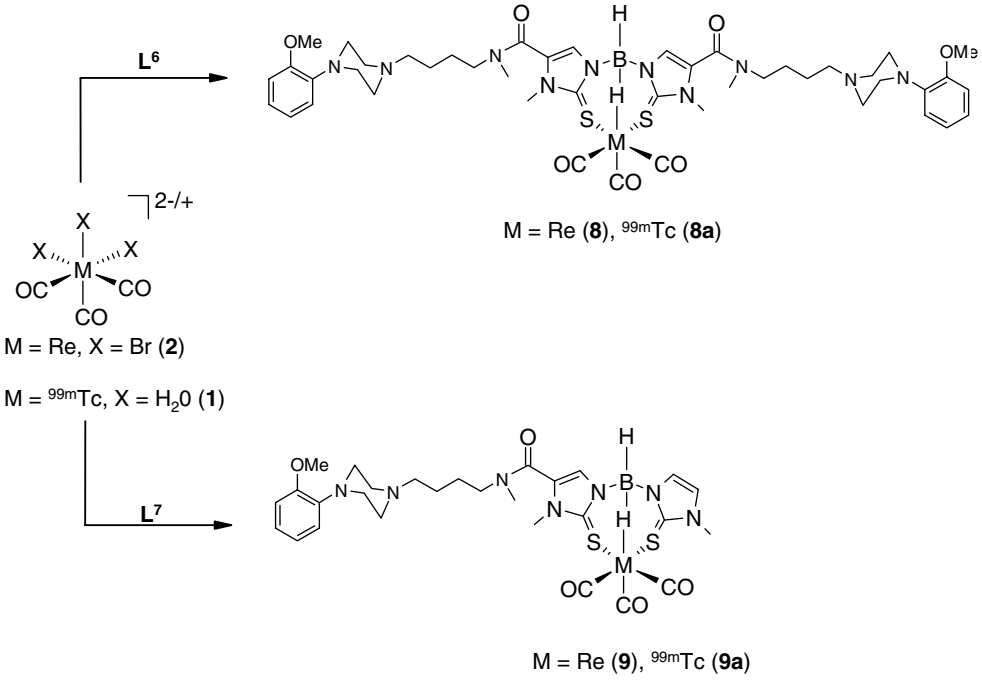

fast-limit exchange ^{1}H NMR spectrum was obtained in CD_3CN (70 °C) with a pattern compatible with the molecular structure of **9**.

The fast-limit exchange spectra show high-field-shifted signals at –6.58 and –6.61 ppm for **8** and **9**, respectively, owing to the protons involved in the B–H···Re agostic interactions. During the variable-temperature NMR studies, the chemical shifts and the shape of these resonances changed only slightly, indicating that the dynamic behaviour of **8** and **9** is not related to the agostic interaction.

By lowering the temperature, we observed the broadening and splitting of some resonances; however, no coalescence process could be unambiguously identified. We were only able to follow the behaviour of the resonances due to the imidazolyl N-CH_3 and to the N-CH_3 amide protons of the $tim^{Bu\text{-}pip}$ fragment, as exemplified for **8** in Fig. 3.

The dynamic behaviour of **8** and **9** can be accounted for by the interconversion of different rotamers, as a consequence of the presence of tertiary amide groups in the ligand backbone [32]. Usually, this interconversion is slow on the NMR timescale, even at room temperature, and separate NMR signals can be observed for the different rotamers. However, the introduction of bulky C or N substituents on the amide function can diminish the barrier to rotation [32]. Apparently, this seems to be the case for **8** and **9**, since their eventual rotamers already undergo a fast interconversion at room temperature.

Complexes **8** and **9** were used as surrogates of the corresponding ^{99m}Tc complexes described later, and were also used to measure the affinity and selectivity towards the 5-HT_{1A} receptors. As can be seen in Table 3, **8** and **9** exhibit IC_{50} values of 0.172 ± 0.003 and 0.71 ± 0.02 nM, respectively. These excellent subnanomolar affinities for the 5-HT_{1A} receptors are among the best values reported for Re and Tc complexes [13]. Moreover, both compounds display moderate to good selectivity against 5-HT_{2A} receptors, with 5-HT_{2A}-to-5-HT_{1A} ratios of 895 and 62 for **8** and **9**, respectively.

Synthesis and biological evaluation of target-specific ^{99m}Tc complexes

The excellent in vitro biological properties exhibited by the target-specific rhenium complexes prompted us to prepare the ^{99m}Tc congeners, aiming to evaluate their interest as radioactive probes for imaging 5-HT_{1A} receptors. As depicted in Scheme 4, complexes **8a** and **9a** were efficiently prepared by reacting **1** with $\mathbf{L^6}$ and $\mathbf{L^7}$ (ligand concentration of 10^{-4} mol L^{-1}) at 75 °C for 30 min. Complex **8a** was obtained with excellent radiochemical purity, typically higher than 95%, and was used without further purification for in vitro and in vivo studies. Complex **9a** was obtained with a radiochemical purity of 80%, owing to the formation of **4a** which resulted from the slight contamination of $\mathbf{L^7}$ with $\mathbf{L^2}$ (see before). After HPLC

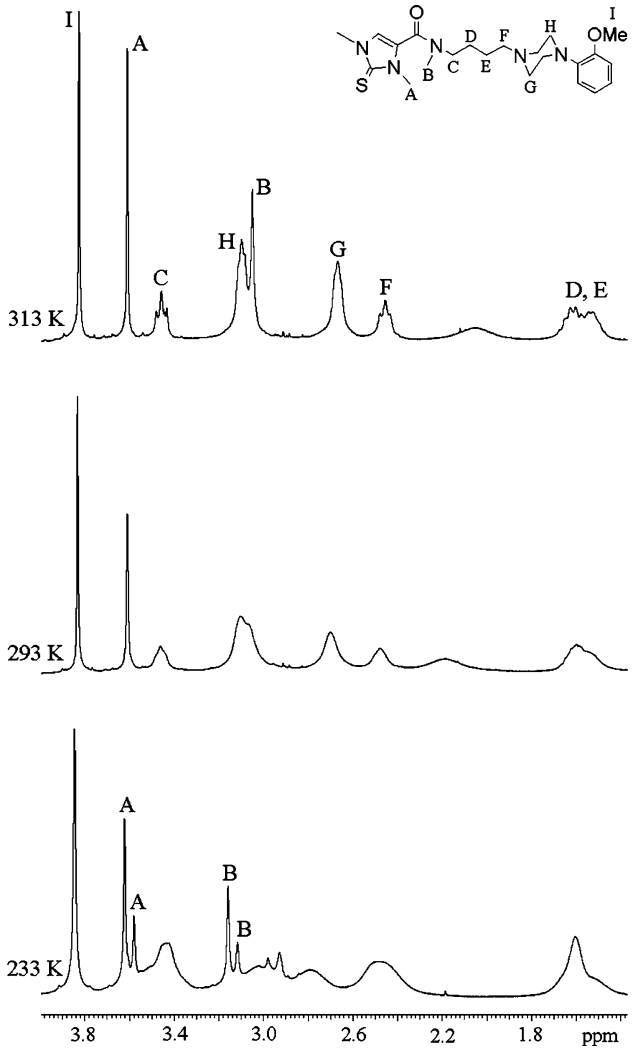

Fig. 3 Variable-temperature ^{1}H NMR spectra of *fac*-[Re{κ^3-H(μ-H)(tim$^{Bu\text{-}pip}$)$_2$}(CO)$_3$] (**8**) (tim$^{Bu\text{-}pip}$ is methyl[4-((2-methoxyphenyl)-1-piperazinyl)butyl](2-mercapto-1-methylimidazol-5-yl)methanamide), in the region of the aliphatic protons

purification, **9a** was also evaluated in vitro and in vivo.

The chemical identification of **8a** and **9a** was done by comparison of their HPLC chromatograms with the HPLC profile of the Re analogues, as shown for **8a** in Fig. 4. Retention times and log$P_{o/w}$ values of **8a** and **9a** are given in Table 4.

Table 3 Inhibition constants (IC_{50}) of *fac*-[Re{κ^3-H(μ-H)(tim$^{Bu\text{-}pip}$)$_2$}(CO)$_3$] (**8**) (tim$^{Bu\text{-}pip}$ is methyl[4-((2-methoxyphenyl)-1-piperazinyl)butyl](2-mercapto-1-methylimidazol-5-yl)methanamide) and *fac*-[Re{κ^3-H(μ-H)B(tim^{Me})(tim$^{Bu\text{-}pip}$)}(CO)$_3$] (**9**) for 5-HT$_{1A}$ and 5-HT$_{2A}$ receptors from rat brain homogenates

Complex	IC_{50} (nM)	
	5-HT$_{1A}$ [^{3}H]OH-DPAT	5-HT$_{2A}$ [^{3}H]ketanserin
8	0.172 ± 0.003	154 ± 3
9	0.71 ± 0.02	44 ± 0.7

The in vitro stability studies of **8a** and **9a**, in PBS, human plasma or challenge experiments with histidine and cysteine, demonstrated that both complexes behave as the parent building block (**4a**). Compounds **8a** and **9a** also remained intact in PBS and in human plasma, after 24 h incubation at 37 °C. After 1 h of incubation at 37 °C, roughly 70% of **8a** and **9a** resisted *trans* chelation with histidine, but only 40–50% of the complexes remained intact towards cysteine challenge.

Biodistribution studies of **8a** and **9a** were performed in female CD-1 mice, to check if these complexes could cross the BBB. The distribution of **8a** and **9a** for most relevant organs is summarized in Table 5.

Complexes **8a** and **9a** show an overall biological profile similar to the one found for the corresponding building block (**4a**). The most striking difference is the slower blood clearance of the target-specific complexes, **8a** and **9a**, in comparison with that for **4a**. Compounds **8a** and **9a** still cross the BBB, displaying a moderate initial brain uptake (1.38 ± 0.46 and 0.43 ± 0.12%ID g^{-1} for **8a** and **9a**, respectively). However, in comparison with **4a**, **8a** and **9a** undergo a relatively rapid washout, with the activity retained in the brain being 0.04 ± 0.01 (**8a**) and 0.18 ± 0.04%ID g^{-1} (**9a**), 60 min after intravenous administration.

The serum of mice injected with **8a** and **9a** was analysed by HPLC, after adequate separation from total blood. Although the formation of a more hydrophilic metabolite (t_R=15.9 min) was observed, complexes **8a** and **9a** are the dominant species in the

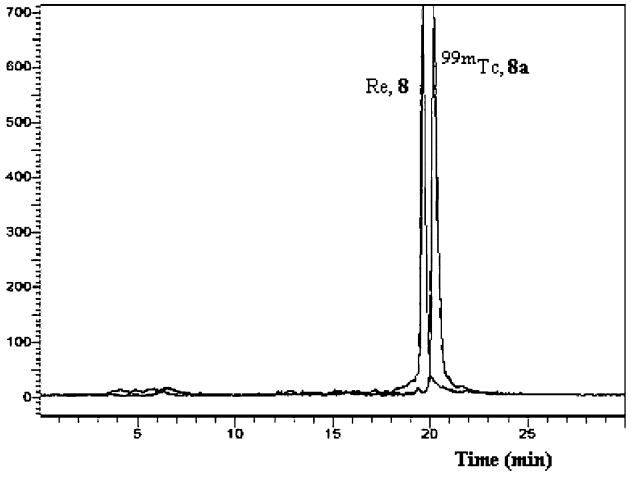

Fig. 4 Comparative HPLC chromatograms of complexes **8** (UV detection) and *fac*-[^{99m}Tc{κ^3-H(μ-H)(tim$^{Bu\text{-}pip}$)$_2$}(CO)$_3$] (**8a**) (radiometric detection)

Table 4 High-performance liquid chromatography retention time (t_R) and log$P_{o/w}$ values for *fac*-[^{99m}Tc{κ^3-H(μ-H)B(tim$^{Bu\text{-}pip}$)$_2$}(CO)$_3$] (**8a**) and *fac*-[^{99m}Tc{κ^3-H(μ-H)B(tim^{Me})(tim$^{Bu\text{-}pip}$)}(CO)$_3$] (**9a**)

Complex	t_R (min)	log$P_{o/w}$
8a	20.0 (19.6)[a]	2.1 ± 0.2
9a	19.5 (18.9)[a]	2.11 ± 0.06

[a]The values in *parentheses* are for the Re complexes **8** and **9**

Table 5 Biodistribution data of complexes **8a** and **9a** in Charles River mice at 5, 60 and 120 min p.i. (%ID g^{-1} ± standard deviation)

Time (min)	Brain	Blood	Liver	Kidneys
Complex **8a**				
5	1.38 ± 0.46 (1.13 ± 0.41)[a]	14.03 ± 3.04	33.37 ± 3.27	8.32 ± 1.44
15	0.30 ± 0.11 (0.18 ± 0.11)[a]	6.37 ± 1.36	35.11 ± 5.96	6.85 ± 0.39
60	0.04 ± 0.01 (<0.01)[a]	3.67 ± 0.46	38.92 ± 2.16	9.13 ± 0.74
Complex **9a**				
5	0.43 ± 0.12 (0.30 ± 0.06)[a]	9.20 ± 0.66	22.63 ± 2.79	13.14 ± 0.72
60	0.16 ± 0.04 (0.10 ± 0.04)[a]	3.48 ± 1.12	24.70 ± 1.36	6.65 ± 0.05

[a]Brain uptake values after correction with ^{99m}Tc-DTPA activity retained in brain

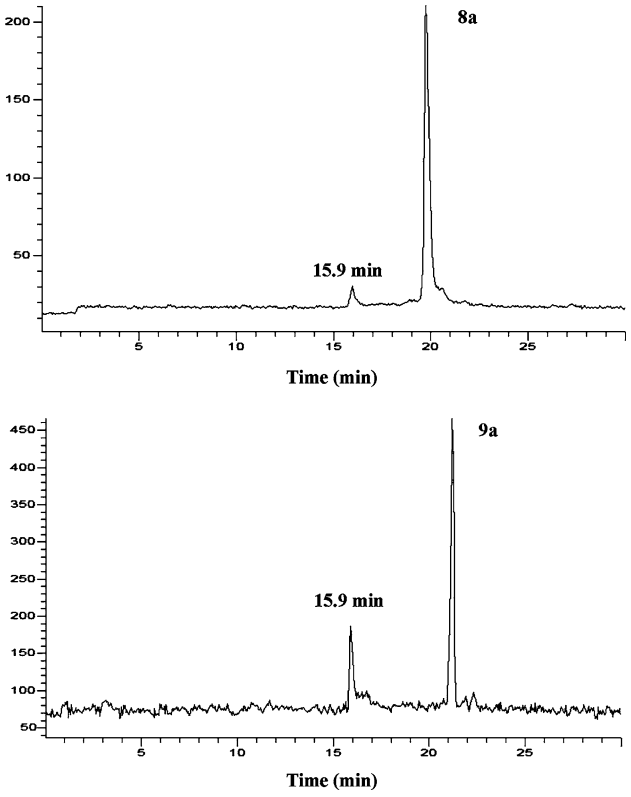

Fig. 5 HPLC analysis of murine serum injected with **8a** and **9a**, at 5 min p.i

bloodstream. This metabolite represents 6.4 (**8a**) and 28.9% (**9a**) of the serum activity at 5 min p.i. (Fig. 5).

Discussion

The design of ^{99m}Tc complexes capable of selectively targeting 5-HT$_{1A}$ receptors is a quite exigent task because the covalent coupling of the targeting biomolecule to a given technetium core must be done with retention of its biological specificity, and the final ^{99m}Tc complex needs to freely cross the intact BBB. Since the introduction of the *fac*-[M(CO)$_3$]$^+$ (M is Re, ^{99m}Tc) moiety, several Werner and/or organometallic type ligands have been explored in the synthesis of ^{99m}Tc complexes for imaging 5-HT$_{1A}$ receptors [15–18]. Within this organometallic approach and profiting from our long experience in the coordination chemistry of boron-containing ligands [33, 34], we have evaluated the utility of Re and Tc(I) tricarbonyl complexes anchored by poly(azolyl)borates for radiopharmaceutical applications. We have anticipated that these types of ligands could be attractive anchors to stabilize ^{99m}Tc tricarbonyl complexes for targeting CNS receptors, owing to their denticity, charge and versatility. Additionally, these ligands could provide an easy tuning of the stability and/or pharmacokinetics of the respective organometallic complexes, by changing the nature (mercaptoimidazolyl vs pyrazolyl) and number (n=2 or 3) of the azolyl rings and by coupling different alkyl/aryl groups to the boron atom. Being negatively charged at physiologic pH, poly(azolyl)borates are not expected to cross the BBB; therefore, they cannot compete with the complexes to target CNS receptors.

Our studies with the poly(pyrazolyl)borates, **L**^{4} and **L**^{5}, have shown that the reactions are not clean, leading to a mixture of species. From NMR spectroscopy, it was clear that some of these species were anchored by heteroscorpionates and/or pyrazole/pyrazolide ligands. In our hands, and starting from compound **2**, the previously described complex **6** [29] could never be isolated and/or identified in the reaction mixture. During this study, the only complex identified was **7**, in which the metal is anchored by a heteroscorpionate containing an N_2O donor atom set (Scheme 2). The formation of this complex results most probably from partial hydrolysis of **L**^{5}, after coordination to the metal. In situ formation of this type of heteroscorpionate, by the action of adventitious water or alcohols, is a well-

documented process in the coordination chemistry of poly(pyrazolyl)borates. The compounds [Ni{BBN(pz)(OH)}(*o*-tol)(PPh_3)] (BBN is 1,5 borabicyclo [3.3.1]nonane]) and [$ReH_4\{\kappa^3$-H(μ-OR)B(3,5-Me_2pz)$_2$}(PPh_3)] (R is Me, Et) are some other examples of transition metal complexes stabilized by heteroscorpionates, formed by hydrolysis or alcoholysis of the original bis(pyrazolyl)borate ligands [35, 36]. At NCA level, our results have shown that compound **1** reacts with $\mathbf{L^4}$ or $\mathbf{L^5}$ to give radiochemical species (t_R=22.5 min) which do not correspond to compounds **6** (t_R=26.2 min) or **7** (t_R=24.1 min). This behaviour indicates that most probably the species formed are ^{99m}Tc tricarbonyl complexes anchored by pyrazole/pyrazolide ligands, formed upon degradation of $\mathbf{L^4}$ or $\mathbf{L^5}$. These data agree with the behaviour observed at the macroscopic level and with results recently reported by Abram et al. [37].

In contrast, the studies performed with poly(mercaptoimidazolyl)borates have shown that these ligands form well-defined complexes, both with Re (**3–5**) and with ^{99m}Tc (**3a–5a**). The resulting complexes are neutral and lipophilic, with the ancillary ligands acting as tridentate ligands in all of them. This coordination mode is, in some cases, achieved through M···H–B agostic interactions (**4**/**4a**, **5**/**5a**). These interactions are completely stable in aqueous solution, in serum, in PBS and even in the presence of large amounts of chloride. A relatively low protein binding has been found for all the complexes, which is a favourable feature of our building blocks, in terms of their application in the design of ^{99m}Tc agents for imaging of CNS receptors. Although we are aware that protein binding can be a reversible process, it is important that the major part of the circulating radioactivity corresponds to free complexes, since they can only cross the BBB in this form.

Challenge experiments have shown that complexes **4a** and **5a** reacted more readily with cysteine than with histidine. This trend can be considered relatively anomalous, since histidine is a more powerful ligand than cysteine towards the *fac*-[^{99m}Tc(CO)$_3$]$^+$ moiety [38]. In our opinion, the enhanced reactivity of **4a** and **5a** with cysteine may indicate an attack of this amino acid on the M···H–B agostic hydride and not a *trans*-chelation process.

The biodistribution profile of **3a–5a** was encouraging, in terms of blood clearance, stability in blood and initial brain uptake. Complex **4a** showed the best ability to cross the BBB. Since all the complexes display similar lipophilicity (log$P_{o/w}$ in the range 1.50–1.64), this behaviour reflects certainly **4a** having the smallest size. In the same animal model, the initial brain uptake for **4a** (1.07 ± 0.11%ID per organ at 5 min p.i.) is comparable to the value reported for ^{99m}Tc-L,L-ethylene dicysteine diethyl ester (ECD) (1.3 ± 0.1%ID per organ at 2 min p.i.), a radiopharmaceutical in clinical use for brain perfusion studies [39].

The coupling of a bioactive fragment to the building block **4a** was performed using a carboxylic function appended at the 5-position of the azole ring. We have previously applied this strategy in the synthesis of the complex *fac*-[Re{κ^3-H_2B(tim^{pip})$_2$}(CO)$_3$] (tim^{pip} is [4-(2-methoxyphenyl)-1-piperazinyl)](2-mercapto-1-methylimidazol-5-yl)methanamide), which showed an unacceptably low affinity (IC_{50}=8,130 ± 505 nM) for the 5-HT_{1A} receptors [40]. The loss of affinity could be attributed to the direct coupling of the piperazinyl moiety to the azolyl ring. Hence, we decided to introduce a butylenic spacer, expecting to improve the affinity to the receptors [16]. To achieve this goal we focused on timH$^{Bu\text{-}pip}$. This compound was previously labelled with ^{11}C, affording a radioligand with excellent subnanomolar affinity and selectivity for 5-HT_{1A} receptors (5-HT_{1A}, IC_{50}=0.86 ± 0.02 nM; 5-HT_{2A}, IC_{50}=480 ± 10 nM) [27].

Taking advantage of the nature of bis(mercaptoimidazolyl)borates, we prepared ligands carrying one ($\mathbf{L^6}$) or two ($\mathbf{L^7}$) functionalized azole rings, by reacting sodium borohydride with timH$^{Bu\text{-}pip}$ or with an equimolar mixture of timH$^{Bu\text{-}pip}$/timH^{Me}. The functionalization of the mercapto(imidazolyl)borates did not compromise their coordination capability towards the *fac*-[M(CO)$_3$]$^+$ moiety and we succeeded in the synthesis of **8**, **8a**, **9** and **9a**. By introducing two pharmacophores per complex, we intended to explore the so-called bivalent ligands approach, one of the methods applied by medicinal chemists in the search for more potent and selective receptor subtype ligands. Since its first application by Portoghese in the field of opioid research, this concept has been successfully applied in the design of agonists or antagonists of several G protein-coupled receptors [41], namely serotonin receptors [42], although radioligands for CNS have remained unexplored.

Competitive receptor binding assays demonstrated that the functionalized rhenium complexes, **8** and **9**, display excellent subnanomolar affinity for the 5-HT_{1A} receptors, confirming the importance of a spacer between the piperazinyl moiety and the bifunctional chelator. Interestingly, the complex bearing two pharmacophores shows the best affinity and selectivity. This seems to indicate that the so-called bivalent ligands approach can improve the biological properties of this family of complexes, where the framework of the bis(mercaptoimidazolyl)borate can be seen as a linker between the two biologically active piperazinyl fragments.

The ^{99m}Tc complexes **8a** and **9a** show a biological profile comparable to the one found for the corresponding building block (**4a**), albeit having a slower blood clearance, most probably owing to the higher molecular weight and/or greater lipophilicity of **8a** and **9a**. In spite of their increased molecular weight, both complexes show a moderate initial brain uptake (1.38 ± 0.46 and 0.43 ± 0.12%ID g^{-1} for **8a** and **9a**, respectively). To confirm that these values were not only due to the residual activity in brain capillaries, we estimated the amount of activity in these blood vessels using ^{99m}Tc-DTPA, a well-established radiotracer that does not cross the BBB. Then, the corrected values for the initial brain uptake were 1.13 ± 0.41 and 0.30 ± 0.04%ID g^{-1} for **8a** and **9a**, respectively. These results confirm the ability of the complexes to cross the BBB, certainly owing to their moderate lipophilic character (**8a**, $\log P_{o/w}=2.1 \pm 0.2$; **9a**, $\log P_{o/w}=2.11 \pm 0.06$) [43]. However, the relatively fast brain washout suggests that **8a** and **9a** may not be promising radioactive probes for in vivo imaging of 5-HT_{1A} receptors, in spite of the excellent in vitro affinity showed by the rhenium counterparts.

Unexpectedly, compound **8a** with the highest molecular weight, owing to the presence of two pharmacophores per ligand, has shown the greatest ability to penetrate into the brain. The molecular weight of **8a** is above the 400–600 threshold that is usually considered for an efficient crossing of the BBB [44]. Although exceptions to this molecular weight rule are not unprecedented [44, 45], it was pertinent to hypothesize that eventual metabolites could be the species effectively penetrating into the brain. To discard this possibility, the serum of mice injected with **8a** and **9a** was analysed by HPLC. This study demonstrated that both complexes undergo some metabolic degradation, forming a more hydrophilic metabolite, but the intact complexes are the dominant species. If the hydrophilic metabolite was responsible for the radioactivity measured in the brain, a greater initial brain uptake would be expected for **9a**. As we just observed the opposite behaviour, **8a** and **9a** must be the radiochemical entities that are effectively penetrating into the brain. This is also corroborated by the hydrophilic character of the detected metabolite, which is not expected to facilitate its free diffusion through the BBB.

Conclusions

We have shown that the monoanionic tris(mercaptoimidazolyl)borates or bis(mercaptoimidazolyl)borates are quite powerful tripodal ligands towards the *fac*-$[^{99m}Tc(CO)_3]^+$ moiety, coordinating to the metal in a (κ^3- H,S,S′) (**3a**, **4a**) or in a (κ^3-S,S′,S″) (**5a**) fashion. The resulting complexes are neutral, lipophilic ($\log P$=1.50–1.64) and are obtained with high radiochemical purity and high specific activity, being also stable in human plasma. In vivo studies have shown that **3a**–**5a** cross the BBB, do not oxidize in vivo and are mainly excreted through the hepatobiliary system. Compound **4a** was chosen to pursue the studies as it presents a reasonable brain uptake at 5 min p. i. (2.40 ± 0.32%ID g^{-1}), which compares well with the values found for the commercially available ^{99m}Tc-L,L-ECD in the same animal model [39]. The properties of **4a** make this building block especially suited for the labelling of CNS receptor ligands, as, for example, arylpiperazine analogues. The conjugation of an arylpiperazine pharmacophore to the 5-position of the azole ring, through a butylenic spacer, allowed the synthesis of well-characterized and stable Re and Tc tricarbonyl complexes anchored on bis(mercaptoimidazolyl)borates containing one (**8**/**8a**) or two (**9**/**9a**) pharmacophores. The affinity and selectivity of the Re complexes to the 5-HT_{1A} subclass of serotonergic receptors were excellent, but the brain uptake of the ^{99m}Tc complexes was relatively low, presenting also a relatively fast washout. The increase of the molecular weight after conjugation of the pharmacophores to the building block **4a** may explain the decrease on the brain uptake.

Acknowledgements This work was partially supported by the FCT (POCTI/QUI/42939/2001). We thank Mallinkrodt-Tyco for financial support. R.G. and L.M. would like to thank the Fundação para a Ciência e Tecnologia (National Foundation for Science and Technology) for Ph.D. and postdoctoral research grants, respectively. We wish to acknowledge Ana Coelho from the Laboratório de Espectrometria de Massa at the Instituto de Tecnologia Química e Biológica, Universidade Nova de Lisboa, Portugal, for the ESI–MS analysis.

References

1. Johannsen B, Pietzsch H (2002) Eur J Nucl Med 29:263–275
2. Passchier J, Waarde AV (2001) Eur J Nucl Med 28:113–129
3. Ito H, Halldin C, Farde L (1999) J Nucl Med 40:102–109
4. Oikonen V, Allonen T, Nagren K, Kajander J, Hietala J (2000) Nucl Med Biol 27:483–486
5. Rabiner EA, Gunn RN, Wilkins MR, Sargent PA, Mocaer E, Sedman E, Cowen PJ, Grasby PM (2000) Nucl Med Biol 27:509–513
6. Andrée B, Halldin C, Thorberg S-O, Sandell J, Farde L (2000) Nucl Med Biol 27:515–521
7. Kung HF, Bradshaw JE, Chumpradit S, Zhuang Z-P, Kung M-P, Mu M, Frederick D (1995) In: Nicolini M, Bandoli G, Mazzi U (eds) Technetium and Rhenium in chemistry and nuclear medicine, SGEditoriali, Padua, pp 293–298

8. Mahmood A, Kronauge JF, Barbaric E, Freiberg E, Madras BK, Li J, Davison A, Jones AG (1999) In: Nicolini M, Bandoli G, Mazzi U (eds) Technetium, Rhenium and other metals in chemistry and nuclear medicine, vol 5. SGEditoriali, Padua, pp 393–399
9. Vanbilloen H, Cleynhens B, Crombez D, Verbruggen A (1999) In: Nicolini M, Bandoli G, Mazzi U (eds) Technetium, Rhenium and other metals in chemistry and nuclear medicine, vol 5. SGEditoriali, Padua, pp 479–484
10. Papagiannopoulou D, Pirmettis I, Maina T, Pelecanou M, Nikolopoulou A, Chiotelis E, Raptopoulou CP, Vlahos AT, Terzis A, Papadopoulos M, Chiotelis E (2001) J Biol Inorg Chem 6:256–265
11. Correia JDG, Domingos A, Santos I, Spies H (2001) J Chem Soc Dalton Trans 2245–2250
12. Fernandes C, Correia JDG, Gano L, Santos I, Seifert S, Spies H, Syhre R (2005) Bioconjugate Chem 16:660–668
13. Drews A, Pietzsch H-J, Syhre R, Seifert S, Varnäs K, Hall H, Halldin C, Kraus W, Karlsson P, Johnsson C, Spies H, Johannsen B (2002) Nucl Med Biol 29:389–398
14. Bolzati C, Mahmood A, Malagò E, Ucelli L, Boschi A, Jones AG, Refosco F, Duatti A, Tisato F (2003) Bioconjugate Chem 14:1231–1242
15. Wald J, Alberto R, Ortner K, Candreia L (2001) Angew Chem Int Ed Engl 40:3062–3066
16. Bernard J, Ortner K, Spingler B, Pietzsch H-J, Alberto R (2003) Inorg Chem 42:1014–1022
17. Palma E, Correia JDG, Domingos A, Santos I, Alberto R, Spies H (2004) J Organomet Chem 689:4811–4819
18. Alberto R, Schibli R, Egli A, Schubiger PA, Abram U, Kaden TA (1998) J Am Chem Soc 120: 7987–7988
19. Metzler-Nolte N (2001) Angew Chem Int Ed Engl 40:1040–1043
20. Sogbein OO, Merdy P, Morel P, Valliant JF (2004) Inorg Chem 43:3032–3034
21. Garcia R, Paulo A, Domingos A, Santos I, Ortner K, Alberto R (2000) J Am Chem Soc 122:11240–11241
22. Garcia R, Paulo A, Domingos A, Santos I (2001) J Organomet Chem 632:41–48
23. Garcia R, Paulo A, Domingos A, Santos I (2003) J Chem Soc Dalton Trans 2757–2760
24. Reglinski J, Garner M, Cassidy ID, Slavin PA, Spicer MD, Armstrong DR (1999) J Chem Soc Dalton Trans 2119–2126
25. Alvarez HM, Tran TB, Richter MA, Alyounes DM, Rabinovich D, Tanski JM, Krawiec M (2003) Inorg Chem 42:2149–2156
26. Trofimenko S (1967) J Am Chem Soc 89:3170–3177
27. Garcia R, Xavier C, Paulo A, Santos I, Torsten K, Bergmann R, Wüst F (2005) J Labelled Compd Radiopharm 48:301–315
28. Alberto R, Schibli R, Egli A, Schubiger PA., Herrmann WA, Artus G, Abram U, Kaden TA (1995) J Organomet Chem 493:119–127
29. Joachim JE, Apostolidis C, Kanellakopulos B, Maier R, Marques N, Meyer D, Müller J, Matos AP, Nuber B, Rebizant J, Ziegler ML (1993) J Organomet Chem 448:119–129
30. Troutner DE, Volkert WA, Hoffman TJ, Holmes RA (1984) Int J Appl Rad Isot 35:467–470
31. Bond A, Green M (1971) J Chem Soc A 682–685
32. Lefrançois L, Hébrant M, Tondre C, Delpuech JJ, Berthon C, Madic C (1999) J Chem Soc Perkin Trans 2:1149–1158
33. Paulo A, Correia JDG, Campello MPC, Santos I (2004) Polyhedron 23:331–360
34. Santos I, Paulo A, Correia JDG (2005) Top Curr Chem 252:45–84
35. Klaüi W, Turkowski B, Rheinwald G, Lang H (2002) Eur J Inorg Chem 205–209
36. Paulo A, Ascenso J, Domingos A, Galvão A, Santos I (1999) J Chem Soc Dalton Trans 1293–1300
37. Kückmann TI, Abram UZ (2004) Anorg Allg Chem 630:783–785
38. Schibli R, La Bella R, Alberto R, Garcia-Garayoa E, Ortner K, Abram U, Schubiger PA (2000) Bioconjugate Chem 11:345–351
39. Vanbilloen HP, Cleynhens BJ, Verbruggen AM (1998) Nucl Med Biol 25:569–575
40. Garcia R, Xing Y-H, Paulo A, Domingos A, Santos I (2002) J Chem Soc Dalton Trans 4236–4241
41. Portoghese PS (2001) J Med Chem 44:2259–2269
42. Tamiz AP, Zhang J, Zhang M, Wang CZ, Johnson KM, Kozikowski AP (2000) J Am Chem Soc 122:5393–5394
43. Gupta SP (1989) Chem Rev 89:1765–1800
44. Pardridge WM (1998) J Neurochem 70:1781–1792
45. Hirohashi T, Terasaki T, Shigetoshi M, Sugiyama Y (1997) J Pharmacol Exp Ther 280:813–819